Nuclear Materials and Energy 13 (2017) 90–98

Contents lists available at ScienceDirect

Nuclear Materials and Energy

journal homepage: www.elsevier.com/locate/nme

Assessment of industrial nitriding processes for fusion steel applications

M. Seitz[a,*], J. Hoffmann[a], M. Rieth[a], P. Margraf[b], R. Senn[b], M. Klimenkov[a], R. Lindau[a], S. Baumgärtner[a], U. Jäntsch[a], P. Franke[a], A. Möslang[a]

[a] Karlsruhe Institute of Technology, Institute for Applied Materials, 76344 Eggenstein-Leopoldshafen, Germany
[b] Härterei Gerster AG, 4622 Egerkingen, Switzerland

ARTICLE INFO

Article history:
Received 15 March 2017
Revised 30 May 2017
Accepted 31 May 2017
Available online 30 June 2017

Keywords:
EUROFER
Nitriding
ODS-EUROFER
Fatigue
Transmission electron microscope (TEM)
Charpy impact tests (DBTT)

ABSTRACT

The 9Cr steels EUROFER and F82H-mod are the candidate materials for future fusion reactors. The extension of the operation limits including temperature, strength and toughness are still the scope of ongoing research. In a pulsed reactor operation, fatigue lifetime is one of the major properties for the steels. While the oxide dispersion strengthened EUROFER-ODS variant showed significant improvements in this area, the production costs and availability of large quantities of materials drastically limits its applications.

In the present study, different surface nitriding treatments of EUROFER972 have been performed and the impact on microstructure, dynamic fracture toughness and high temperature fatigue has been analysed. Four different states of EUROFER including different heat treatments, nitriding of the surface and the ODS variant are tested and compared in this work.

Low cycle fatigue tests show the improvements after certain treatments. Charpy impact tests and microstructural investigation by scanning electron microscopy and analytical transmission electron microscopy are also performed to compare the materials against the reference (EUROFER97).

While conventional gas nitriding showed no beneficial effect on the material, the Hard-Inox-P treatment showed a significant improvement in the cycles to failure while retaining an acceptable toughness. Microstructural investigations showed the presence of very small chromium- and nitrogen-rich precipitates in the area close to the surface.

Introduction

9Cr reduced activation ferritic martensitic steels (RAFM) are foreseen as the main structural steels for future fusion reactors beyond ITER. Development of these classes of materials started in the early to mid-1990s across several research associations in Europe, Japan and in the United States of America. Inspired by the class of 9Cr steels such as grade P91 and P92 used in conventional and nuclear fission applications, the materials were developed towards low activation and high irradiation tolerance under neutron irradiation [1–5]. EUROFER97 and its variants have been heavily investigated in the recent years. This has led to the availability of a large set of properties which includes code qualified data for a EU RAFM database with multiple records for tensile, impact, fracture toughness and fatigue lifetime [6].

Advanced breeding concepts demand for an extension of the temperature range from 350 °C – 550 °C (conventional EUROFER97) to 350 °C – 650 °C. These requirements lead to the fabrication of the oxide dispersion strengthened (ODS) variant of EUROFER97 [7]. Fine dispersed Y_2O_3 particles inside the matrix increase strength and creep resistance but lead to a loss in fracture toughness [8]. The fatigue properties also benefit from the strengthening ODS particles. The cyclic stresses nearly double compared to conventional EUROFER97 while the cyclic softening is suppressed. The cycles to failure is also shifted to higher numbers [9,10]. Generally the literature data on fatigue of 9Cr ODS steels are scarce and would benefit from more experiments for a more thorough investigation of the underlying mechanisms [9–11]. The initial fatigue results on ODS steels indicate already [10] that at lower strain amplitudes the dislocations are no longer able to overcome the nanoscaled ODS particles. Consequently, the mean free path of dislocations is strongly reduced and the formation of sufficiently long in- and extrusions that become later nanocracks at the surface, is strongly retarded. Much longer fatigue lifetimes are the natural consequence.

* Corresponding author.
E-mail address: michael.seitz@kit.edu (M. Seitz).

http://dx.doi.org/10.1016/j.nme.2017.05.015

From these findings it may also be derived more generally that the goal to increase the fatigue life-time could in principle be satisfied by the condition to increase substantially the density of any stable small obstacles on the glide planes of dislocations. Therefore, the major attempt of the present investigation was to validate whether nitride particles introduced into the surface of cast steels could provide also a remarkable increase of the fatigue lifetime. An eventual (partly) substitution of ODS steels by an alternative technology would be very beneficial as the fabrication process of high quality ODS steels is complex and the overall availability of large quantities of materials is limited.

The nitriding of steel is a state-of-the-art technique to modify and harden the surfaces for improved wear resistance, corrosion resistance and fatigue lifetime [12,13]. It is especially common for high-alloyed austenitic steels where martensitic hardening of the outer layers is not possible. Studies which applied hardening surface treatments (diamond-like-carbon layer) observed an increase in fatigue lifetime due to the comprehensive stresses in the crack initiation zone caused by the hardened outer layer in constant amplitude loading [14]. In addition, if applied accordingly, the nitriding treatments are capable of producing nanoscaled intermetallic phases (chromium-nitride). Such chromium and nitrogen rich precipitates may work as crack arrestor for micro cracks in the early stages of the fatigue [15]. The existence and geometry of these small cracks are the dominant factor for fatigue damage and they are more important than other microstructural properties such as dislocation structure or overall fracture toughness [16].

The need for extended operation windows for EUROFER97 and the downsides of the ODS materials motivated the present work. Nitriding of the surfaces of finished and semi-finished parts of RAFM steels may give rise to a compromise of the two classes of materials. The authors intend to demonstrate the potential of the surface treatments to significantly improve fatigue lifetime with only minor sacrifices to other properties. All measured effects of the nitriding layer on mechanical and microstructural properties will be compared against EUROFER97 and EUROFER-ODS.

Experimental details

Material

In this study four different surface and heat treatment conditions were examined (two pure heat treatments and two nitriding processes). The base material of each of these conditions was the heat 993402 of the European reference steel for fusion applications EUROFER97-2. The chemical composition of this batch is 8.89% Cr, 0.18% V, 1.06% W, 0.53% Mn, 0.15% Ta, 0.037% N and 0.096% C (in wt.%). The investigation of the reference material is listed in [17].

The requirement of a rapid radioactive decay behavior does not allow the use of some elements such as nickel, cobalt and molybdenum which are common in conventional high-temperature materials. These have to be substituted by elements which satisfy the requirements regarding the mechanical properties and do not degrade the decay noticeably. After a period of 100 years after the end of irradiation, nitrogen significantly influences the activity of RAFM steels by the decay of ^{14}C, which is formed by neutron irradiation. However, the influence on the equivalent dose is negligibly small in the case of nitrogen contents present in the materials treated within this work, since the proportion of energy to be released per decay, in contrast to other elements, is very small.

A chromium content of about 9% allows martensitic hardening without leading to segregations at longer exposure times at high temperatures. Vanadium and tantalum form high temperature resistant precipitates (carbides and nitrides) that inhibit prior austenite grain growth and increase the high temperature strength. The proportion of 1% tungsten is a compromise between increased strength on the one hand and the breeding ratio of the blanket and acceptable toughness values on the other hand [7,18].

Table 1 lists the finally applied heat treatments and nitriding processes which were investigated in this work.

The two selected heat treatments were chosen according to different characteristics. HT1 should have increased strength while the focus of HT2 is on high ductility and toughness. The high austenitizing temperature was chosen to increase creep strength.

The aim of the two nitriding processes (gas nitriding and Hard-Inox-P) is to improve mechanical properties such as strength and fatigue behavior without losing ductility. For nitriding, the samples were sent to Gerster (Egerkingen, CH) in a quenched and tempered condition. Here the first method was gas nitriding. At a temperature of 550 °C the samples were exposed to a nitrogen environment (N_2 and NH_3 with the nitriding potential $N_k = 3$) for 36 hours. Subsequent cooling also took place in nitrogen atmosphere. The following annealing at 750 °C in vacuum ensures comparability with other states. A further discussion of the materials in this state is omitted, since all characteristic properties remain significantly behind those of the reference material. The second method was the Hard-Inox-P method, which is a proprietary nitriding process from the portfolio of the company Gerster [19]. In this case, high-temperature nitriding is performed at 1050 °C for a period of one hour in a vacuum furnace under a nitrogen partial pressure of 500 mbar. Quenching under nitrogen atmosphere to −80 °C and a freezing of one hour at that temperature is followed by a final heat treatment at a temperature of 750 °C in vacuum.

For an approximate determination of the nitrogen content after the Hard-Inox-P method, the phase diagram shown in Fig. 1 was calculated using the Thermocalc database TCFe7. The expected components in the equilibrium state are plotted as a function of the nitrogen content. This may give insight on the phases, which could form during the process. The mass fraction of nitrogen is approximately 0.3% for the above-mentioned process parameters of the Hard-Inox-P process (1050 °C, 500 mbar). Given the fact that the phase diagram is only valid for equilibrium conditions, these concentrations may only be applicable for the boundary layers.

The chemical composition of EUROFER ODS steel is slightly different from that of the other samples. The following elements were alloyed to iron: 8.9% Cr, 1.1% W, 0.2% V, 0.14% Ta, 0.42% Mn, 0.06% Si, 0.11% C. The mechanical alloying with Y_2O_3 was realized by an industrial ball milling at PLANSEE SE, Reute, Austria. The two examined ODS steels differ in their content of oxide particles of 0.3 wt.% and 0.5 wt.% [7,8]. Subsequently, the powder was molded by hot isostatic pressing into bars with a diameter of 60 mm and a length of 300 mm.

Testing program

The mechanical testing program comprised fatigue tests, Charpy impact tests and Vickers hardness measurements for the characterization of the surface layer.

The fatigue tests were performed on two universal testing machines under vacuum ($\leq 4 \times 10^{-5}$ mbar). The strain rate in all experiments was $\dot{\varepsilon} = 0.1\%/s$. Dwell time at the reversal points of the loading cycles was half a second. Monitoring of the test temperature of 550 °C was carried out at three points to ensure a homogeneous temperature distribution. The test was stopped at a stress level lower than 30% compared to the first cycle.

Hardness measurement of the surface layer with HV0.1 was required to characterize the surface layer of the nitrided samples. The measurements were carried out and evaluated by an instrumented hardness testing machine. The impact tests were conducted by an instrumented Charpy machine with an automated sample tempering and loading mechanism.

Table 1
Investigated heat treatments.

Designation	Heat treatment			
	Previous treatment/austenitization		Tempering	
	T (°C)	t (min)	T (°C)	t (min)
Reference material	980	30	760	90
Heat treatment 1 (HT1)	1150	30	700	120
Heat treatment 2 (HT2)	1150	30	750	120
Gas nitriding	HT1		Nitriding (550 °C/36 h) & 750	120
Hard-Inox-P	Hard-Inox-P (1050 °C/1 h)		750	120
ODS-EUROFER [7]	Hot isostatic pressing			
	1100	30	750	120

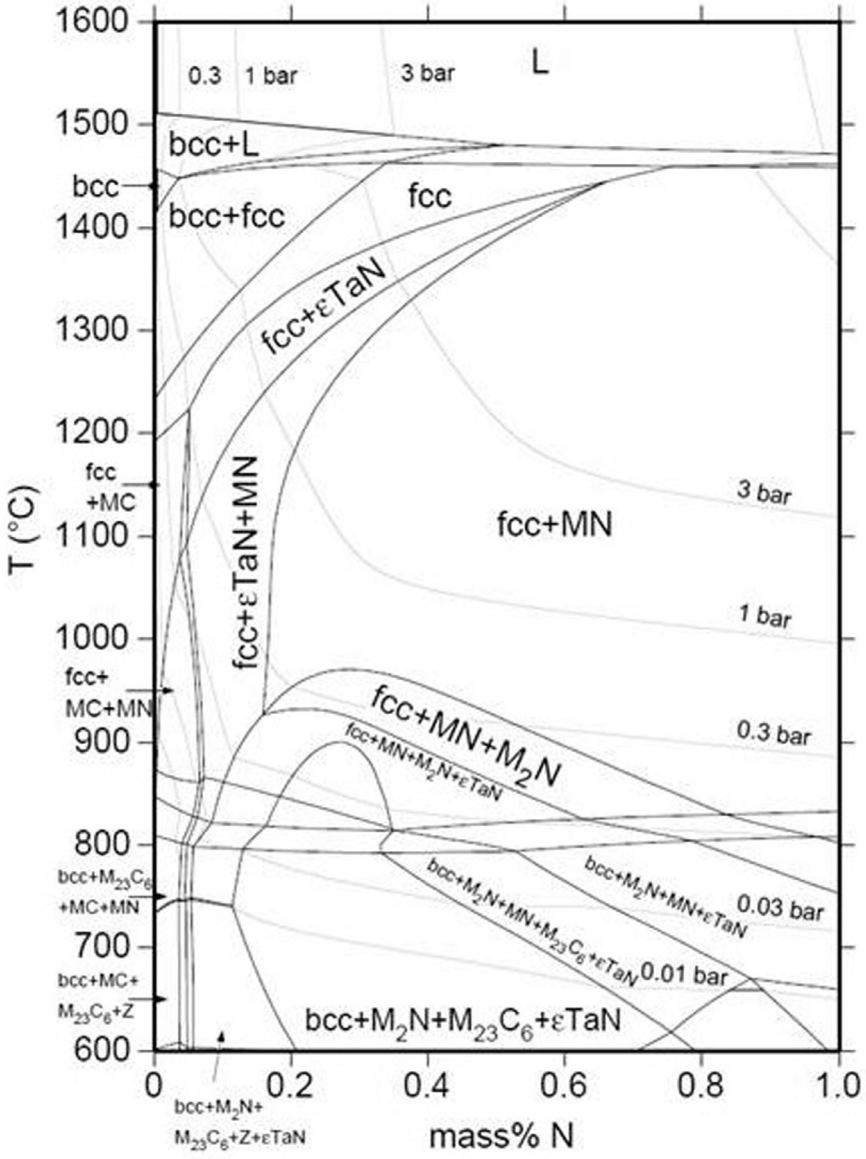

Fig. 1. Phase diagram of EUROFER in dependence of the nitrogen content.

For the fatigue tests SSCS (small size cylindrical specimen) were used [20]. The cylindrical sample geometry with a diameter of 2 mm and a gauge length of 7.6 mm was originally designed for use in IFMIF (International Fusion Materials Irradiation Facility). The comparability of the results with standard samples was validated by various material models in finite element calculations [21] (see [20]). To have a greater resistance to crack initiation, the surface of the LCF samples were ground in axial direction to an average roughness R_a of 0.262 ± 0.033 µm.

The geometry of the KLST Charpy impact test specimens is specified in the standard DIN 50115 [22]. The length of the sample is 27 mm, the cross-section measures 3 mm x 4 mm. The notch angle is 60° with a depth of 1 mm and a radius of 0.1 mm. The samples were machined in L-S direction.

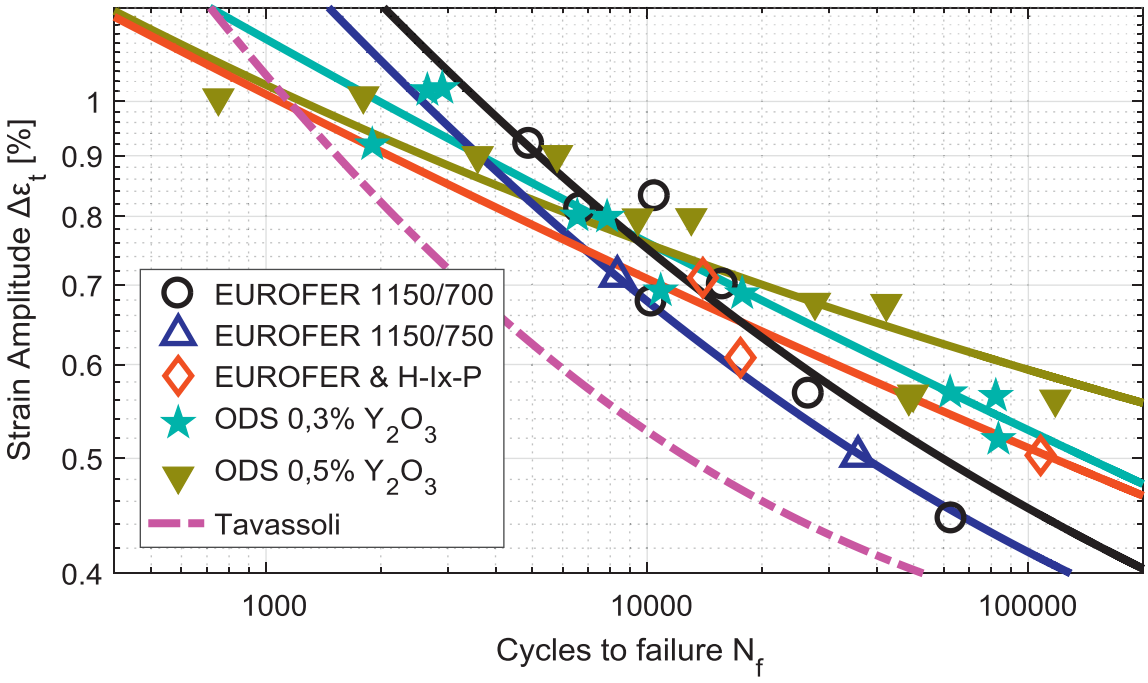

Fig. 2. Endurance of EUROFER 97 at 550 °C for different heat and surface conditions.

The microscopic studies were performed of the cross sections of the tested KLST samples and of the LCF longitudinal sections. For scanning electron microscopy both the SEM "XL30 ESEM" with a LaB6 cathode FEI and the Zeiss "Merlin" with a field emission gun were used. For the chemical analysis of the boundary layer regions an EDAX Trident systems consisting of an Octane Super SDD EDS detector and a LEXS WDS detector was utilized. The preparation steps included mechanical grinding and polishing up to a mirror finish and a brief etching with a mixture of 400 ml ethanol, 50 ml nitric acid, 50 ml hydrochloric acid and 5 gr picric acid. A FEI Tecnai F20 transmission electron microscope (TEM) with a field emission gun operating at 200 kV and an EDS detector was used for the materials characterization on nanoscale level. A specimen for TEM characterization was prepared using lift-out lamella produced on a Cross Beam Workstation (FIB-SEM), ZEISS Auriga. The area investigated by TEM had a distance of 10 µm from the sample surface.

Results and discussion

Fatigue tests at 550 °C

To describe the number of cycles to failure the evaluation of fatigue tests according to Manson, Coffin and Basquin was chosen (formula (1)). The elastic and plastic characteristics at 0.5 N_f were evaluated to determine the parameters.

$$\Delta\varepsilon_A = \Delta\varepsilon_e + \Delta\varepsilon_p = \frac{\sigma_f'}{E}(2N_f)^b + \varepsilon_f'(2N_f)^c \quad (1)$$

The elastic component of the equation consists of the fatigue strength coefficient σ_f', the Young's modulus E and the fatigue strength exponent b. The cyclical ductility coefficient ε_f' and the cyclic ductility exponent c describe the plastic part. The number of cycles to failure is denoted by N_f.

Fig. 2 shows the number of load cycles to failure depending on the applied load. In addition to the heat treated and nitrided EUROFER samples, the results of Tavassoli [23] and the ODS variant of EUROFER are presented. Obviously, there is an increase in the life time compared to the values of Tavassoli who has summarized many fatigue tests on EUROFER in a temperature range from 500 °C to 550 °C from various research institutions for code qualification.

When applying a lower tempering temperature, service lifetime is prolonged for all tested strain amplitudes. Thus, for heat treatment 1, the average lifetime is extended by a factor of 1.7 for related strain levels compared to heat treatment 2. The largest life extension could be achieved with the Hard-Inox-P treatment at low total strain amplitudes. This behavior is caused by fine precipitates in the near surface area, which pin small microcracks. However, for larger loads these precipitates can act as micro notches which promote the damage caused by cyclic loading. The same behavior is shown by the two ODS steels, which again show an increase in life time compared to the Hard-Inox-P treated samples for low loads. The higher the proportion of yttrium, the more pronounced is this behavior. The increase in lifetime of the two alloys with HT1 and HT2 compared to the Tavassoli data can possibly be explained by a hardness increase in the matrix which inhibits crack initiation. Also, the summarized literature data on EUROFER fatigue are averaged and represent a conservative image of the lifetime.

Cyclic softening

Fig. 3 shows the softening behaviour of EUROFER in the initial state, after Hard-Inox-P treatment and with ODS particles at a total elongation of 0.7%.

The results of [24–26] show that after about 100 cycles the softening coefficient is independent of the applied strain amplitude of EUROFER. This behavior was only observed by the authors after the second heat treatment at 500 cycles and at the Hard-Inox-P Method after 1000 cycles. The description of the cyclic softening can be presented by formula (2):

$$\sigma_A = A \cdot N^{-s} \quad (2)$$

Here σ_A is the stress amplitude, A is a constant, N is the considered cycle and s the cyclic softening coefficient.

Marmy and Kruml [24] and Armas et al. [25] studied LCF tests of EUROFER at a test temperature of 550 °C resulting in the cyclic softening coefficients of 0.0485 and 0.077. The softening coefficients of HT2 with an average of 0.0550 and the Hard-Inox-P

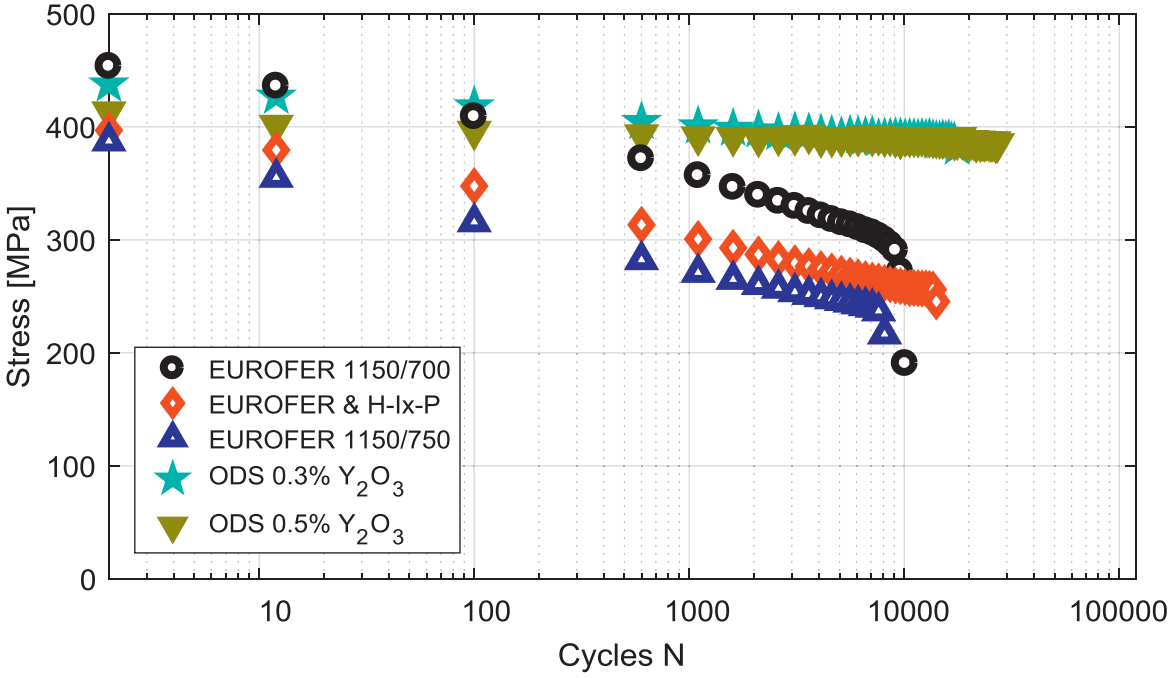

Fig. 3. Comparison of the softening behaviour at a total elongation of 0.7% with different heat and surface conditions at 550 °C.

Table 2
Softening coefficient depending on the total strain amplitude.

Total strain range (%)	Softening coefficient
0,5	0,0382
0,6	0,0475
0,7	0,0543
0,8	0,0603
0,9	0,0607

treated samples with an average of 0.0582 are also in this interval. The softening behavior of the first heat treatment depends significantly on the load as can be seen in Table 2.

The two EUROFER ODS steels do also not follow this law as can be seen in Fig. 3. While the softening is barely recognizable at an oxide content of 0.3%, no softening takes place at a higher oxide content of 0.5%.

A similar good softening behavior could not be achieved by the Hard-Inox-P process. Although the stress drop is not as intense as in the comparative sample, it is more pronounced in case of the ODS steels.

Hardness measurement

The hardness of the reference material was examined by [17] and is 220 HV30. In contrast to expectations and manufacturer's instructions [19] no hardness increase in boundary layer related areas could be measured for the nitration Hard-Inox-P. Irrespective of the distance to the specimen surface the hardness was at 221 HV0.1. The average hardness after the first heat treatment was considerably higher with 316 HV0.1, the second heat treatment showed a hardness value of 252 HV0.1. The divergence between the hardness values of the two heat treatments can be explained by the different tempering temperature and has frequently been investigated [17]. The even lower hardness of the Hard-Inox-P treated samples may result from the lower austenitizing temperature.

Charpy impact tests

The characteristics of the dynamic fracture toughness are given in Fig. 4. In addition to the first heat treatment and the Hard-Inox-P treated samples, the reference curve of EUROFER after a heat treatment of 980 °C and 760 °C (similar to HT2), as well as two different ODS alloys are shown. The determination of the DBTT was carried out by fitting the individual measurements with hyperbolic tangent curve according to the formula:

$$K = a + b*\tanh\left(\frac{T - T_0}{c}\right) \quad (3)$$

Here K describes the impact energy, a is the mean and b is half the distance between USE (Upper Shelf Energy) and LSE (Lower Shelf Energy). T_0 indicates the transition temperature and c the temperature ranges of transition. The determination of the parameters of this approach was carried out with a least squares fit. Table 3 shows the determined DBTT of all experiments:

The DBTT of conventional EUROFER is adjustable just by a different heat treatment in a range from -120 °C to 51 °C. Similar results were found in the work by [27] with a slightly lower DBBT shift of 100 K. Similarly, the upper shelf energy (USE) is reduced by 10% after tempering at a lower temperature. In addition, the transition area between USE and lower shelf energy has been increased by tempering at a lower temperature.

By applying Hard-Inox-P process, the transition temperature shifts by 40 K to −81 °C influenced by the nanoscale precipitates in the surface layer, which will be described later. This method narrows the transition region. This leads to a similar behaviour as the reference batch 993402. The DBTT of the two ODS EUROFER steels resembles that of the first heat treatment, but showing a lower maximum impact energy. Consequently, at a low tempering temperature EUROFER loses significantly in toughness. The nanoscale particles in EUROFER-ODS deteriorate the resistance to dynamic stress. Treating the samples with the Hard-Inox-P method leads to only a slight displacement of the DBTT.

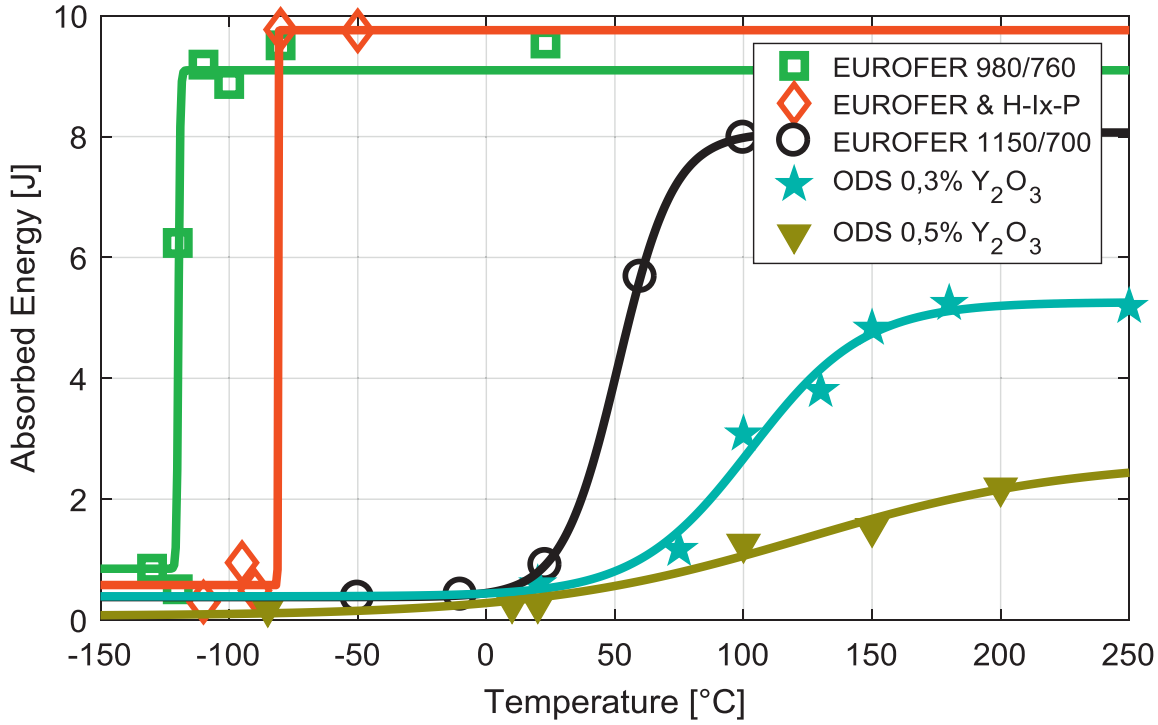

Fig. 4. Comparison of the absorbed energy after Charpy testing.

Table 3
DBTT of the tested conditions.

	EUROFER 980/760 (Reference)	EUROFER Hard -Inox-P	EUROFER 1150/700 (HT1)	ODS 0,3% Y_2O_3	ODS 0,5% Y_2O_3
T_0 (°C)	−120	−81	51	103	124

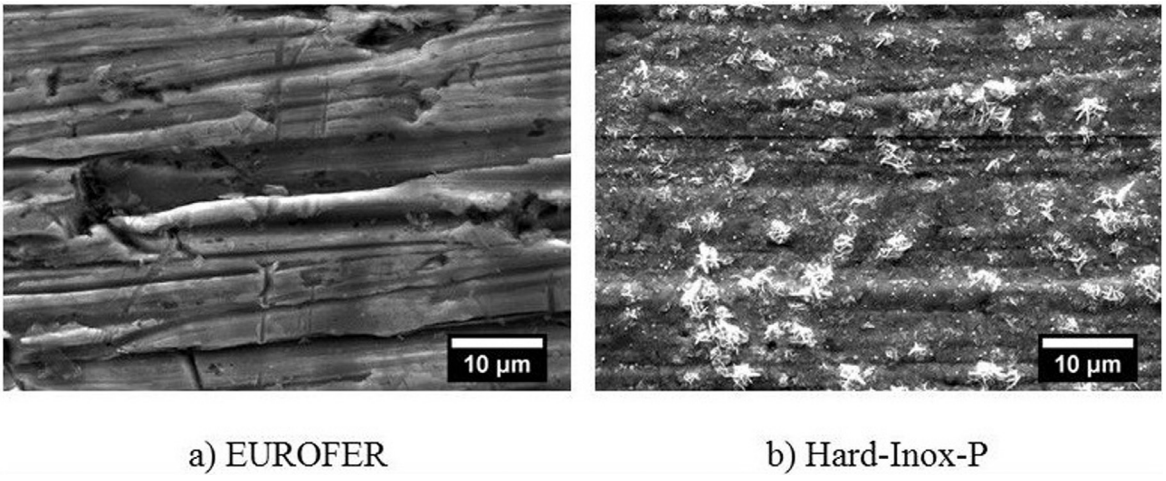

Fig. 5. Image of the surface to characterize the influence of the Hard-Inox-P process.

Microscopy

The difference of the surface finish by Hard-Inox-P treatment is documented in the electron micrographs in Fig. 5. The surface of the initial EUROER material after longitudinal polish shows distinct grinding marks in the longitudinal direction (a) while the Hard-Inox-P method (b) reduces the severity of the scratches. Instead, small bright tiles in different density arrays decorate the surface. The roughness was slightly improved by nitriding, as roughness measurements showed.

The prior austenite grain boundaries cannot be seen in the micrograph of the sample with Hard-Inox-P treatment. Instead, martensitic laths are dispersed and unstructured over the entire cross-sectional area as the optical micrograph in Fig. 6(a) documents. To answer the question of the effect of the high-temperature nitrogen method on the structure of the surface layer, the other images at higher magnifications give an insight. The recording with a magnification of 1500× by a secondary electron detector are shown in Fig. 6(b). The lath structure of the martensite can still be recognized in the form of many distributed precipitates near the surface. The two images 6(c) and (d) are taken with the

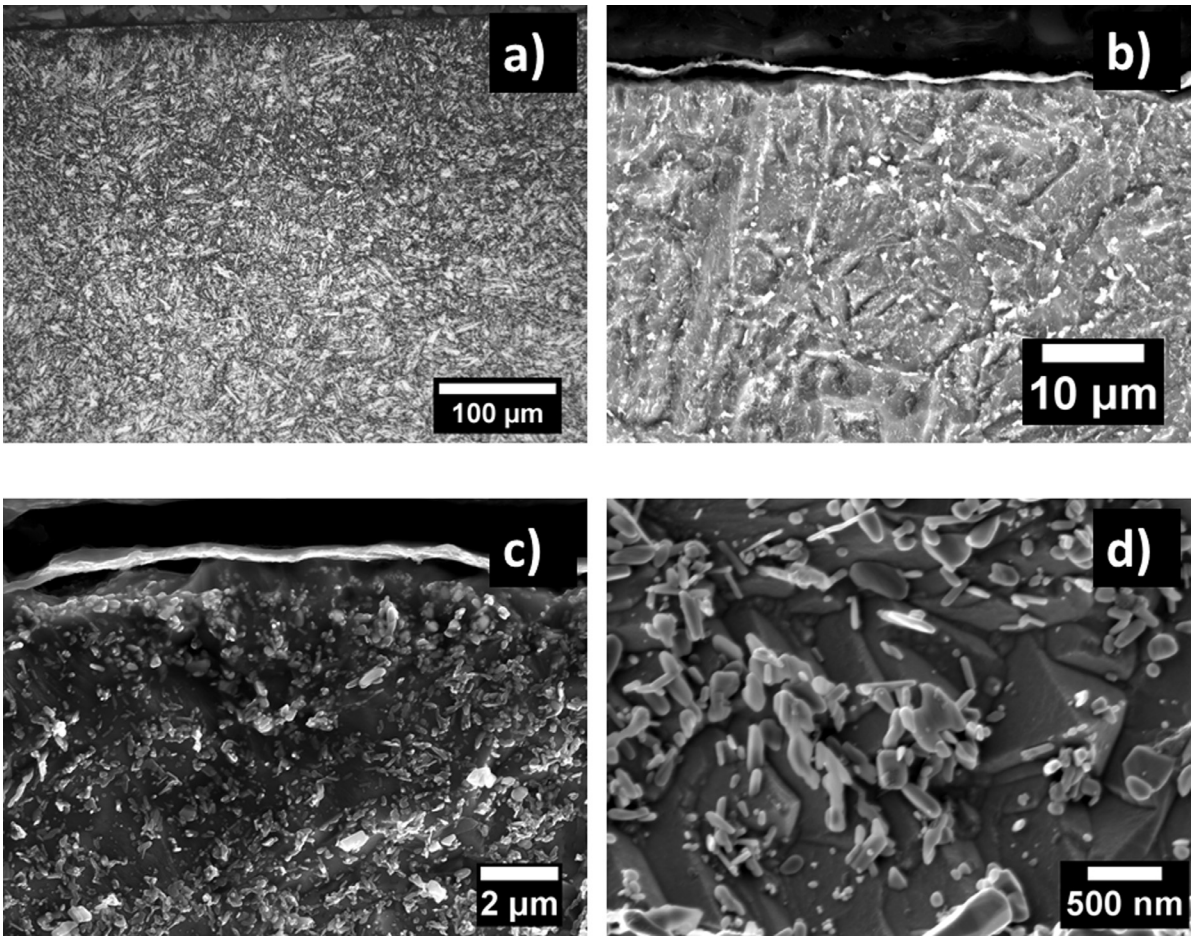

Fig. 6. Microstructure of the boundary layer of EUROFER after Hard-Inox-P treatment.

InLens detector and have a variety of finely dispersed, nanoscale precipitates with platelet and rod structure on the surface of the metallographic cut. Besides some larger precipitations, diverse precipitates less than 50 nm are visible. The penetration depth of the smallest precipitates was determined by further micrographs with increasing margin to about 100 µm.

To better determine the distribution of elements in the edge region, the energy-dispersive x-ray spectroscopy (EDS) was used. For the determination of the nitrogen distribution over the edge of the sample the wavelength dispersive X-ray spectroscopy (WDS) was applied, which has a higher detection sensitivity than the energy-dispersive X-ray spectroscopy. Fig. 7 indicates that after the Hard-Inox-P treatment boundary layers show a lower concentration of iron (a) associated with the establishment of higher chromium content (c). A correlation of the nitrogen distribution and the chromium precipitates cannot be made on the basis of these measurements as the comparison of images (b) and (c) illustrates. A noticeable local increase of the nitrogen content is not apparent from the WDS measurement. However, very finely divided rashes based on small white and gray dots especially in the boundary area are visible. This implies that the above-described nanoscale precipitates are mainly nitrides and that the measurement of carbon in the entire edge area did not exceed the detection sensitivity.

The nitrogen influence on formation of precipitates was studied using 2-dimensional EDX elemental mapping (Fig. 8) in TEM. The distribution of all relevant compositional elements is shown in the maps (b–g). Two different kind of precipitates were detected in total: a Cr-rich $M_{23}C_6$ phase with $(Cr,Fe,V)_{23}(C,N)_6$ composition and a MN phase with (V,Ta)N composition. Remarkable is that N is present in all precipitates. The size of the $M_{23}C_6$ particles (100–250 nm) is larger than in EUROFER97 without N addition [12]. Their distribution is well visible in the Cr map, part (c). The MN phase is well visible in the Ta map (e), because Ta is not contained in the $M_{23}C_6$ particles. This phase was detected as pure nitride. The presence TaC phase, which is typical for EUROFER97, was not detected.

Conclusions

The mechanical characteristics of EUROFER may be varied by heat treatment within a broad range as shown by the comparison above. The material of the heat treatment 1 (HT1) with a tempering temperature of 700 °C is stronger and harder as the mechanical tests show. The toughness decreases substantially as the increase in DBTT demonstrates. Life expectancy increases in contrast.

The second heat treatment with a tempering temperature of 750 °C has a lower time to failure and a lower hardness. However, the DBTT is below −100 °C, as the Charpy impact tests show for a similar heat treatment.

The two ODS steels show an additional lifetime increase for smaller loads and nearly no softening at all. Though as the ODS particle fraction increases, the lifetime for smaller loads (below 0.8%) and the resistance to softening are increased. In contrast, a higher proportion of particles has a negative effect on the dynamic cracking toughness as shown by the Charpy impact tests. A solution that combines both advantages has not yet been found even if an approximation could be achieved [7,8].

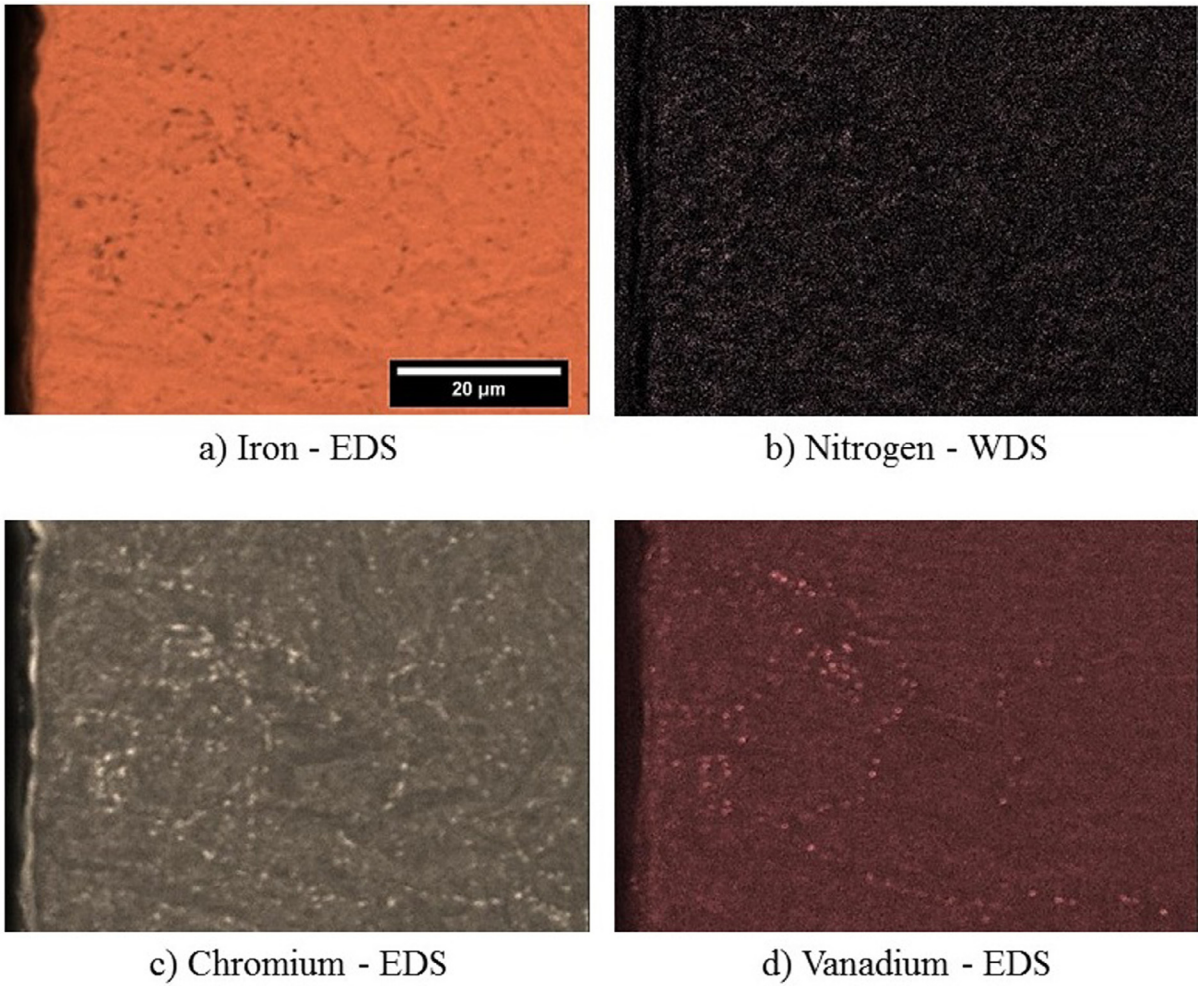

Fig. 7. Chemical analysis of the boundary layer after Hard-Inox-P treatment.

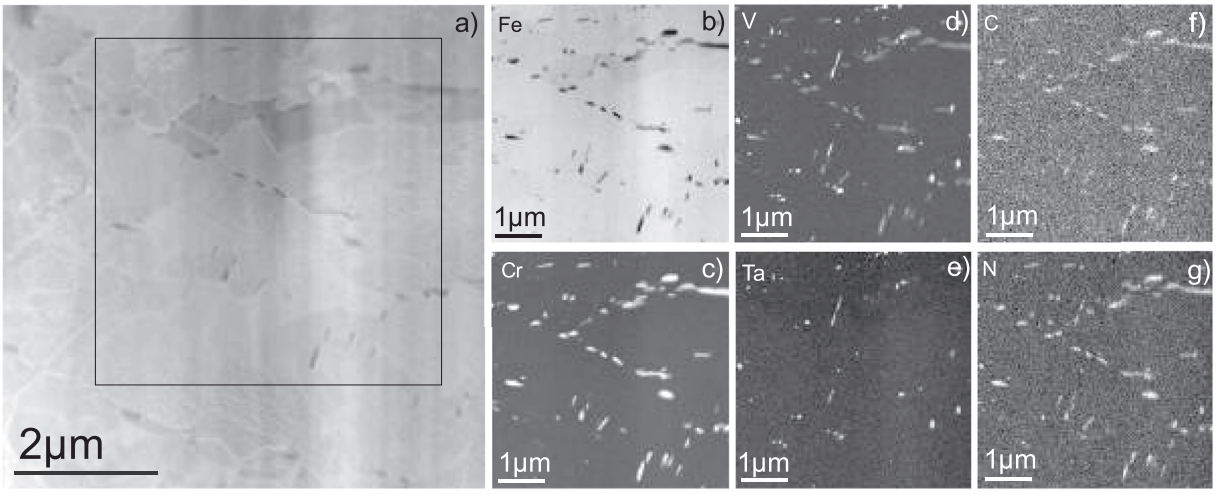

Fig. 8. Analytical investigations of precipitates in N–rich region. The dark field image shows an investigated area (a), and Fe, Cr, V, Ta, C and N 2-dimensional elemental maps are presented in parts (b–g).

The high temperature nitriding process Hard-Inox-P demonstrates a longer lifetime in particular at low loads (0.5%) in comparison to the two heat treatments and an acceptable loss in fracture toughness towards the reference material. The strength is increased slightly with a DBTT shift of 40 K. Furthermore, SEM and TEM images show the formation of $M_{23}C_6$ and fine MN precipitations, which may be responsible for the positive influence on the mechanical characteristic values. The advantage of Hard-Inox-P compared to ODS steels lies in the manufacturing. The Hard-Inox-P method is already state of the art as well as significantly cheaper and simpler. Thus, this procedure is promising for future fusion applications.

For EUROFER, with the chosen process parameters and sample geometry, gas nitriding is unsuitable for the requirements of dura-

bility and toughness. Whether an adjustment of these variables has the desired effect can be doubted about due to the large discrepancy to the reference samples.

Parameter variations of partial pressure, time and temperature profile have to be examined in a next step in order to evaluate the potential of the high temperature nitriding. An extension of the mechanical tests by creep and fatigue tests increases the statistical significance and provides information on further requirements for high-temperature materials in particular in the area of fusion power plants.

Acknowledgement

The authors are grateful to all their colleagues at the Karlsruhe Institute of Technology, M. Hoffmann, D. Bolich and M. Kärcher are especially acknowledged for their contributions. The authors also thank the Gerster AG, Egerkingen for the overall use of their facilities. Furthermore the authors acknowledge support by the German Research Foundation and the Open Access Publishing Fund of Karlsruhe Institute of Technology.

References

[1] R. Klueh, E.T. Cheng, M.L. Grossbeck, E. Bloom, Impurity effects on reduced-activation ferritic steels developed for fusion applications, J. Nucl. Mater. 280 (2000) 353–359.
[2] K. Ehrlich, S.W. Cierjacks, S. Kelzenberg, A Möslang, in: The Development of Structural Materials for Reduced Long-Term Activation, 1270, ASTM Special Technical Publications, STP, 1996, pp. 1109–1122.
[3] G.R. Odette, M.J. Alinger, B.D. Wirth, Recent developments in irradiation-resistant steels, Annu. Rev. Mater. Res. 38 (2008) 471–503.
[4] H. Tanigawa, K. Shiba, A. Möslang, R.E. Stoller, R. Lindau, M.A. Sokolov, G.R. Odette, R.J. Kurtz, S. Jitsukawa, Status and key issues of reduced activation ferritic/martensitic steels as the structural material for a DEMO blanket, J. Nucl. Mater. 417 (2011) 9–15.
[5] J. Knaster, A. Moeslang, T. Muroga, Materials research for fusion, Nat. Phys. 12 (5) (2016) 424–434.
[6] A.-A. Tavassoli, E. Diegele, R. Lindau, N. Luzginova, H. Tanigawa, Current status and recent research achievements in ferritic/martensitic steels, J. Nucl. Mater. 455 (2014) 269–276.
[7] R. Lindau, A. Möslang, M. Rieth, M. Klimiankou, E. Materna-Morris, A. Alamo, A.-A.F. Tavassoli, C. Cayron, A.-M. Lancha, P. Fernandez, N. Baluc, R. Schäublin, E. Diegele, G. Filacchioni, J.W. Rensman, B. Schaaf, E. Lucon, W. Dietz, Present development status of EUROFER and ODS-EUROFER for application in blanket concepts, Fusion Eng. Des. 75-79 (2005) 989–996.
[8] R. Lindau, A. Möslang, M. Schirra, P. Schlossmacher, M. Klimenkov, Mechanical and microstructural properties of a hipped RAFM ODS-steel, J. Nucl. Mater. 307-311 (2002) 769–772.
[9] I. Kuběna, T. Kruml, P. Spätig, N. Baluc, Z. Oksiuta, M. Petrenec, K. Obrtlík, J. Polák, Fatigue behaviour of ODS ferritic-martensitic Eurofer steel, Procedia Eng. 2 (2010) 717–724.
[10] P. He, M. Klimenkov, R. Lindau, A. Möslang, Characterization of precipitates in nano structured 14% Cr ODS alloys for fusion application, J. Nucl. Mater. 428 (2012) 131–138.
[11] S. Ukai, S. Ohtsuka, Low cycle fatigue properties of ODS ferritic–martensitic steels at high temperature, J. Nucl. Mater. 367-370 (2007) 234–238.
[12] W.J. Yang, M. Zhang, Y.H. Zhao, M.L. Shen, H. Lei, L. Xu, J.Q. Xiao, J. Gong, B.H. Yu, C. Sun, Enhancement of mechanical property and corrosion resistance of 316 L stainless steels by low temperature arc plasma nitriding, Surf. Coat. Technol. 298 (2016) 64–72.
[13] S. Ganesh Sundara Raman, M. Jayaprakash, Influence of plasma nitriding on plain fatigue and fretting fatigue behaviour of AISI 304 austenitic stainless steel, Surf. Coat. Technol. 201 (2007) 5906–5911.
[14] H. Kovacı, A.F. Yetim, Ö. Baran, A. Çelik, Fatigue crack growth behavior of DLC coated AISI 4140 steel under constant and variable amplitude loading conditions, Surf. Coat. Technol. 304 (2016) 316–324.
[15] Y. Yamashita, Y. Murakami, Small crack growth model from low to very high cycle fatigue regime for internal fatigue failure of high strength steel, Int. J. Fatigue 93 (2016) 406–414.
[16] Y. Murakami, M.S. Ferdous, C. Makabe, Low cycle fatigue damage and critical crack length affecting loss of fracture ductility, Int. J. Fatigue 82 (2016) 89–97.
[17] E. Materna-Morris, C. Adelhelm, S. Baumgärtner, P. Dafferner, P. Graf, S. Heger, U. Jäntsch, R. Lindau, C. Petersen, M. Rieth, R. Ziegler, H. Zimmermann, Structural material EUROFER97-2, Characterization of Rod and Plate Material: Structural, Tensile, Charpy, and Creep Properties: Interner Bericht, Karlsruhe, 2007.
[18] C.B.A. Forty, Activation response of martensitic steels, J. Fusion Energy 16 (1997) 277–284.
[19] Härterei Gerster AG, HARD-INOX: Fürhöhere Ansprüche an Verschleiss- und Korrosionsbeständigkeit, http://www.gerster.ch/userfiles/downloads/1464001867820950/Brosch%C3%BCre_HARD-INOX_d_web.pdf (accessed 29.07.16).
[20] A. Möslang, E. Diegele, Development of small scale specimens for creep-fatigue testing in irradiation environment, Presented at ICFRM-10, Baden-Baden, 2001.
[21] C. Petersen, V. Shamardin, A. Fedoseev, G. Shimansky, V. Efimov, J. Rensman, The ARBOR irradiation project, J. Nucl. Mater. 307-311 (2002) 1655–1659.
[22] Deutsches Institut für Normung e.V., DIN 50115 - Kerbschlagbiegeversuch, Beuth Verlag, Berlin, 1991.
[23] F. Tavassoli, Eurofer steel, development to full code qualification, Procedia Eng. 55 (2013) 300–308.
[24] P. Marmy, T. Kruml, Low cycle fatigue of Eurofer 97, J. Nucl. Mater. 377 (2008) 52–58.
[25] A.F. Armas, C. Petersen, R. Schmitt, M. Avalos, I. Alvarez-Armas, Mechanical and microstructural behaviour of isothermally and thermally fatigued ferritic/martensitic steels, J. Nucl. Mater. 307-311 (2002) 509–513.
[26] C. Vorpahl, A. Möslang, M. Rieth, Creep–fatigue interaction and related structure property correlations of EUROFER97 steel at 550 °C by decoupling creep and fatigue load, J. Nucl. Mater. 417 (2011) 16–19.
[27] J. Henry, S. Doriot, S. Vincent, C. Caes, C. Toffolon, Improvement of EUROFER 97 high-temperature mechanical properties using non-standard heat treatments, Presented at ICFRM 17, 2015.